Proceedings World Geothermal Congress 2000
Kyushu - Tohoku, Japan, May 28 - June 10, 2000

A SYSTEMATIC APPROACH TO LOCAL GRID REFINEMENT IN GEOTHERMAL RESERVOIR SIMULATION

Karsten Pruess and Julio Garcia

Earth Sciences Division, Lawrence Berkeley National Laboratory
University of California, Berkeley, CA 94720, U.S.A.
K_Pruess@lbl.gov

Keywords: numerical simulation, discretization errors, sharp fronts, enthalpy transients, TOUGH2.

ABSTRACT

Thermodynamic conditions of geothermal reservoir fluids, such as pressures, temperatures, phase compositions, and concentrations of dissolved solids and non-condensible gases, may show strong spatial variability in the vicinity of production and injection wells. Large spatial variations also can occur near reservoir heterogeneities, such as faults and lithologic contacts. In numerical simulation of flow and transport, fine gridding is required to accurately represent steep changes in fluid conditions. This can necessitate prohibitively large numbers of grid blocks in conventional finite difference discretization, where finer gridding is applied globally with reference to a global system of coordinates.

This paper presents a more economical alternative, in which fine gridding is applied only to the regions in which large gradients in thermodynamic conditions need to be resolved. We have implemented a scheme for local grid refinement into the general-purpose geothermal reservoir simulator TOUGH2. We discuss the concept and algorithms used for local grid refinement, as well as applications to production from and injection into fractured two-phase reservoirs. The accuracy and economy of local grid refinement are demonstrated by comparison with globally fine grid simulations.

1. INTRODUCTION

For purposes of numerical simulation the volume of a geothermal reservoir is partitioned into subdomains referred to as "volume elements" or "grid blocks." By discretizing the continuous space coordinates, the governing differential (or integral) equations for flow and transport are replaced by difference equations, which can only provide approximate solutions to the underlying differential equations. Artefacts from space discretization, often called "space truncation errors" (Peaceman, 1977; Aziz and Settari, 1979), can be reduced by means of finer grid spacing. In geothermal reservoir simulation problems the advective terms usually dominate; for these, space discretization errors typically are approximately proportional to grid spacing (Pruess, 1991a). Reducing discretization errors through grid refinement increases the number of grid blocks and increases computational work. The number N of grid blocks in a given reservoir volume V increases with decreasing grid spacing h proportional to $1/h^D$, where D (= 1, 2, 3) is the dimensionality of the flow problem. Computational work for a reservoir simulation increases with number of grid blocks proportional to N^ω, with $\omega \approx 1.4$ - 1.6 for iterative solvers, and $\omega \approx 3$ for direct solvers (Moridis and Pruess, 1998). Improved accuracy for space discretization comes, therefore, at the expense of rapidly increasing computational work, especially for multi-dimensional problems.

The tradeoff between space discretization accuracy and computational work can be improved by increasing grid resolution only in those reservoir regions where thermodynamic conditions may have strong spatial variability, or may change rapidly. To illustrate this point, Fig. 1a shows a coarse 2-D Cartesian grid with 3x4 = 12 volume elements and a production well at the center of one of the grid blocks. A standard method of grid refinement is shown in Fig. 1b, where smaller grid increments Δx and Δy are used to increase spatial resolution in the region containing the well. The grid refinement shown in Fig. 1b, in addition to providing better spatial resolution in the neighborhood of the well, also introduces additional grid blocks in regions that are distant from the well. This will increase computational work without significantly improving numerical accuracy. A better alternative is the "local" grid refinement shown in Fig. 1c, where additional grid blocks are introduced only in proximity to the well. Other conditions where local grid refinement may be advantageous include reservoir regions with strong permeability contrasts, such as fractures or faults, and regions of localized recharge or discharge.

Different techniques for local grid refinement have been discussed in the literature, including "static" methods with time-independent grid refinement (Hermitte and Guerrillot, 1993; Cao and Kitanidis, 1999; Ewing and Lazarov, 1994), and "dynamic" approaches, in which zones of grid refinement are allowed to move in the course of a simulation (Verwer and Trompert, 1993; Trompert, 1995; Schreiber and Kuo, 1998). Hermitte and Guerrillot (1993) applied the static subgridding approach in simulations of isothermal, incompressible, two–phase, 2-D flow in heterogeneous porous media. Dynamic local grid refinement is primarily used to simulate propagation of sharp fronts. Examples include concentration fronts in isothermal, single-phase, 2-D flow in porous media (Verwer and Trompert, 1993; Trompert, 1995), and propagation of a moving melt boundary (Schreiber and Kuo, 1998).

In geothermal reservoir simulation, the typically coarse grids used for field-wide models have been refined by inserting radial grids around wells, to be able to represent near-well boiling and associated enthalpy transients (Pruess et al., 1984). This was done in an ad hoc fashion that is not amenable to quantitative analysis and control of discretization errors. Here we present a systematic approach, in which local grid refinement is made by further partitioning of a regular Cartesian grid system (Fig. 1c). We describe the methods used for subgridding, and present

several examples to demonstrate and evaluate the method for different flow processes, including isothermal and non-isothermal single-phase flow, and two-phase non-isothermal flow with boiling and condensation effects.

2. METHODOLOGY

Fig. 2 shows an enlarged view of a portion of the locally refined grid of Fig. 1c. In our general-purpose geothermal reservoir simulator TOUGH2 (Pruess, 1991b), the pressure gradient that drives fluid flow across the interface between grid blocks 1 and 2 is approximated as

$$(\nabla P)_{12} \equiv (P_1 - P_2)/D_{12} \qquad (1)$$

where D_{12} is the nodal distance between points 1 and 2. The integral finite difference method used in TOUGH2 (Narasimhan and Witherspoon, 1976) requires that the nodal line connecting points 1 and 2 be perpendicular to the interface between the respective grid blocks, in order that Eq. (1) may represent the normal component of the pressure gradient with respect to this interface. In the locally refined grid shown in Fig. 2, a problem now arises in the computation of the pressure gradient at the interfaces between the smaller and larger blocks. In general, nodal lines running from the smaller grid blocks perpendicular to their interfaces with block 2 will not intersect a nodal point on the other side. This situation is remedied by introducing "interpolation nodes" at which the required information can be obtained by spatial interpolation from neighboring grid nodes. For example, Fig. 2 shows an interpolation node labeled "i," which is located at the intersection between the nodal line originating from grid block # 3, and the nodal line between 1 and 2. Fluid pressure at i is obtained by linear interpolation between 1 and 2,

$$P_i = P_2 + (P_1 - P_2)D_{i2}/D_{12} \qquad (2)$$

where D_{i2} is the distance between points i and 2. The normal component of pressure gradient at the interface between blocks 2 and 3 is then written as

$$(\nabla P)_{23} \equiv (P_i - P_3)/D_{i3} \qquad (3)$$

where D_{i3} is the distance between nodes i and 3. The same interpolation scheme is used for other parameters that are needed to calculate mass and heat fluxes at the interface between 2 and 3, including temperature, relative permeability, viscosity, density, enthalpy, capillary pressure, and mass fractions of solutes or non-condensible gases.

Note that fluxes across interfaces between the locally refined and the coarsely gridded regions (as between blocks 2 and 3 in Fig. 2) depend not only on thermodynamic conditions in the grid blocks adjacent to that interface. Because of the interpolation required, there is an additional dependence on thermodynamic conditions in another coarse block (1 in Fig. 2). In our implementation of local grid refinement for 2-D rectangular grids in TOUGH2, we calculate all additional terms in the Jacobian matrix that arise from this dependence, to avoid deterioration in convergence rates.

3. EVALUATION

In this section we discuss the application of the local grid refinement scheme to production from and injection into a geothermal reservoir. The test problem considers a large well field with wells arranged in a "five-spot" pattern with 1080 m well spacing. Because of symmetry only 1/4 of the basic pattern needs to be modeled (Fig. 3). Cold water ($T \approx 20$ °C) is injected at a rate of 15 kg/s (full-well basis), and production occurs at the same rate. The initial pressure, temperature and saturation conditions are P = 100 bars, T = T_{sat}(100 bars) = 311.02 °C, S_{vap} = 0.01. Simulation parameters are presented in Table 1. Due to the injection of cold water, temperature and condensation fronts propagate from the injection well into the reservoir, while vapor saturations increase from boiling around the production well.

In order to compare the accuracy and economy of the local grid refinement scheme we conducted simulations on three computational grids, namely, coarse, fine and locally refined grid (Fig. 4). The coarse grid consists of 81 volume elements with block sizes of 60 m x 60 m. The fine grid is obtained by global refinement around production and injection wells, resulting in 441 volume elements with three different block sizes (60 m x 60 m, 60 m x 20 m and 20 m x 20 m). Finally, local refinement of the coarse grid around the injection and production wells results in a locally refined grid of 225 volume elements with block sizes of 60 m x 60 m and 20 m x 20 m.

Simulation results after 2 years show excellent agreement between the fine and locally refined grids (Fig. 4). At this time, the temperature and saturation fronts have already moved beyond the local refinement regions around the injection and production well. Compared with the fine and locally refined grid simulations, the coarse grid has larger discretization errors and produces more disperse temperature and saturation fields.

A summary of memory and CPU requirements is given in Table 2. All simulations were performed using automatic time stepping, based on the convergence rate of the Newton-Raphson iteration. Time step size is doubled if convergence occurs within 4 or less iterations, and is reduced by a factor 4 if convergence is not achieved within eight iterations. Local grid refinement reduces the size of the Jacobian matrix by 50% with no sacrifice in accuracy relative to the fine grid simulations. The locally refined grid requires only about half the simulation time as the corresponding fine grid.

We also ran problem variations with different initial conditions and for longer simulation times. For two-phase initial conditions, excellent agreement between locally refined and fine grid simulations was found for all parameters in all cases. For single-phase liquid initial conditions, somewhat larger discrepancies were noted when a boiling front moves away from the production well (Garcia and Pruess, in preparation).

4. BOUNDED 2-D RESERVOIR

This problem considers production from a hot two-phase reservoir, with initial conditions of P = 60 bars, T = T_{sat}(60

bars) = 275.55 °C, S_g = 0.01. The reservoir has 4 x 3 = 12 km^2 areal extent, 200 m thickness. The relative permeability functions used are van Genuchten's (1980) function

$$k_{rl}=\sqrt{S^*}\left\{1-\left(1-\left[S^*\right]^{1/\lambda}\right)^{\lambda}\right\}^2 \qquad (4)$$

for the liquid phase and Corey's (1954) function

$$k_{rg}=\left(1-S'\right)^2\left(1-(S')^2\right) \qquad (5)$$

for the gas phase, with the reduced saturations given by $S^*=(S_l - S_{lr})/(1 - S_{lr})$ and $S' = (S_l - S_{lr})/(1 - S_{lr} - S_{gr})$, respectively. Other problem parameters are given in Table 3. For purposes of numerical simulation, a 2-D grid system is used with horizontal block dimensions of 200 m x 200 m, which is a typical grid resolution that would be used for field-wide studies. A coupled reservoir-wellbore simulation is performed for a single production well located at (x, y) = (1300 m, 900 m), to examine flow rate and enthalpy transients for a well producing at constant wellhead pressure from this hot two-phase reservoir.

Simulations with three different grids were performed, namely, (1) a coarse grid with 200 m x 200 m block size, for a total of 20x15 = 300 blocks, (2) a fine grid, in which the intervals 1200 m ≤ x ≤ 1400 m, and 800 m ≤ y ≤ 1000 m, were each subdivided into 11 intervals of 18.18 m each, resulting in a total of 750 grid blocks, and (3) a locally refined grid, in which just the coarse grid block containing the well was partitioned into 11x11 = 121 blocks, for a total of 420 blocks. As a reference case we also performed a simulation for a 1-D radial grid system with the same total area. The radial grid has a fine resolution of 2 m near the well, and gradually (logarithmically) coarsens at larger distance. The productivity index for the well was adjusted as required for the different sizes of the grid blocks containing the well (Thomas, 1982).

The 1-D radial flow simulation has very small space discretization errors, and is viewed as providing the "true" solution to the problem for the time period where no boundary effects are encountered. This simulation shows that at $t = 10^8$ seconds, a small increase in gas saturation, from initial 1 % to 1.5 %, has migrated to a distance of 750 m, so that up to this time both the rectangular reservoir problem and the 1-D radial flow problem are infinite acting.

Results for flow rate and enthalpy transients are shown in Fig. 5. A complex behavior is seen for the 1-D radial case. Well flow rate decreases rapidly initially, as production-induced boiling raises the enthalpy and diminishes the mobility of the produced fluid. After about 2 days, produced enthalpy reaches a maximum, and subsequently both enthalpy and production rate show a slow rate of decline. The non-monotonic behavior of enthalpy arises from "retrograde" condensation: when steam with temperature exceeding that at maximum steam enthalpy (T≈235 °C) flows towards the well, it is subject to adiabatic decompression with formation of condensate. The coarse grid simulation gives very poor results for both flow rates and enthalpies, as had been expected. The fine grid simulation does well for flow rates throughout, but it misses the fairly brief enthalpy maximum. Closer inspection shows that the enthalpy maximum in the radial flow simulation arises from boiling that is localized within a region of a few meters from the well, which is not resolved by the fine grid. The pronounced decline in enthalpy seen in the fine grid simulation after about 10^7 seconds is due to adiabatic decompression effects as lower enthalpy fluids are drawn to the well from beyond the region of finer discretization.

Results for the locally refined grid agree very well with those for the globally fine grid, and are indistinguishable up to $5x10^6$ seconds. The minor differences seen from 10^7 to $2x10^8$ seconds occur because the globally fine grid has smaller grid blocks outside of the locally refined region, which gives slightly reduced discretization errors there. For a simulation time of 10^9 sec, CPU times on an IBM RS/6000 computer were 33.92, 118.67, and 63.00 sec, respectively, for the coarse, fine, and locally refined grid.

5. DISCUSSION AND CONCLUSIONS

A systematic approach for local refinement of 2-D regular grids has been developed and implemented in the TOUGH2 simulator. This makes it possible to accurately resolve spatial variations of thermodynamic conditions over small distances, as occur near production and injection wells. By including all thermodynamic dependencies into the Jacobian matrix, the same convergence rates as for global grid refinement are obtained. Test calculations have shown the method to achieve similar accuracy as globally refined grids, at considerable savings in the number of grid blocks and computing time.

Future work will explore more general grid geometries, including 3-D, and multiple levels of grid refinement.

ACKNOWLEDGEMENT

Thanks are due to M. Lippmann and S. Finsterle for a review of the manuscript. This work was supported by the Assistant Secretary for Energy Efficiency and Renewable Energy, Office of Geothermal and Wind Technologies, of the U.S. Department of Energy under Contract No. DE-AC03-76SF00098.

REFERENCES

Aziz, K. and A. Settari (1979). *Petroleum Reservoir Simulation*, Elsevier, London and New York.

Cao, J. and P.K. Kitanidis (1999). Adaptive-Grid Simulation of Groundwater Flow in Heterogeneous Aquifers, *Advances in Water Resources,* Vol. 22, No. 7, pp. 681 - 696.

Corey, A.T. (1954) The Interrelation Between Gas and Oil Relative Permeabilities, *Produces Monthly*, 38-41.

Ewing, R.E. and R.D. Lazarov (1994). Approximation of Parabolic Problems on Grids Locally Refined in Time and Space, *Applied Numerical Mathematics,* Vol. 14, pp. 199 - 211.

Hermitte, T. and D.R. Guerillot (1993). A More Accurate Numerical Scheme for Locally Refined Meshes in Heterogenous Reservoirs. Proceedings, *12th SPE Symposium on Reservoir Simulation,* pp. 321 - 331, New Orleans, Feb 28-March 3.

Moridis, G. and K. Pruess (1998). T2SOLV: An Enhanced Package of Solvers for the TOUGH2 Family of Reservoir Simulation Codes, *Geothermics*, Vol. 27, No. 4, pp. 415 - 444.

Narasimhan, T.N. and P.A. Witherspoon (1976). An Integrated Finite Difference Method for Analyzing Fluid Flow in Porous Media, *Water Resour. Res.*, Vol. 12, No. 1, pp. 57 – 64.

Peaceman, D.W. (1977) *Fundamentals of Numerical Reservoir Simulation*, Elsevier, Amsterdam, The Netherlands.

Pruess, K. (1991a) Grid Orientation and Capillary Pressure Effects in the Simulation of Water Injection into Depleted Vapor Zones, *Geothermics*, 20 (5/6), 257-277.

Pruess, K. (1991b) TOUGH2 - A General Purpose Numerical Simulator for Multiphase Fluid and Heat Flow, Lawrence Berkeley Laboratory Report LBL-29400, Lawrence Berkeley Laboratory, Berkeley, CA.

Pruess, K., G.S. Bodvarsson, V. Stefansson and E.T. Eliasson (1984). The Krafla Geothermal Field, Iceland, 4, History Match and Prediction of Individual Well Performance, *Water Resour. Res.*, Vol. 20, No. 11, pp. 1561 - 1584.

Schreiber, W. and J. Kuo (1998). A Computational Study of Some Possible Factors Associated with Melt Eruption Events, in: K. Pruess (ed.), Proceedings of the TOUGH Workshop '98, pp. 275 - 280, Lawrence Berkeley National Laboratory Report LBNL-41995, Berkeley, CA.

Thomas, G.W. (1982) *Principles of Hydrocarbon Reservoir Simulation.* International Human Resources Development Corporation, Boston.

Trompert, R. (1995) *Local Uniform Grid Refinement for Time-Dependent Partial Differential Equations,* CWI Tract, Netherlands.

Verwer, J.G. and R.A. Trompert (1993). Analysis of Local Uniform Grid Refinement, *Applied Numerical Mathematics,* Vol. 13, pp. 251 - 270.

van Genuchten, M.Th. (1980) A Closed-Form Equation for Predicting the Hydraulic Conductivity of Unsaturated Soils, *Soil Sci. Soc.* , 44 (892-898).

Table 1. Parameters for five-spot problem.

FORMATION	
Rock Grain Density	2650 kg/m^3
Porosity	25%
Effective Permeability	$1.0*10^{-13}$ m^2
Specific Heat	1000 J/kg°C
Thickness	15 m
Relative Permeability: Corey curves with	$S_{lr} = 0.30$ $S_{vr} = 0.05$
INITIAL CONDITIONS	
Pressure	100 bar
Liquid Saturation	0.99
PRODUCTION/INJECTION	
Pattern Area	1.1664 km^2
Distance between producers and injectors	763.7 m
Production rate(a)	15 kg/s
Injection rate(a)	15 kg/s
Injection enthalpy	100 kJ/kg

(a) full well basis

Table 2. Memory and CPU requirements for the five-spot problem.

Grid	coarse	locally refined	fine
elements	81	225	441
connections	144	432	840
non-zero Jacobian matrix elements	1476	4516	8484
time steps¤	16	20	24
Newtonian iterations¤	64	88	111
CPU-time#	1.26 s	5.38 s	10.88 s

¤ for simulating two years

PC with Pentium® II at 400 MHz

Table 3. Parameters for 2-D reservoir problem.

Reservoir thickness	200 m
Permeability	50×10^{-15} m^2
Porosity	0.05
Relative permeability	
irreducible water saturation	$S_{lr} = 0.15$
exponent	$\lambda = 0.457$
irreducible gas saturation	$S_{gr} = 0.05$
Rock grain density	2600 kg/m^3
Specific heat	1000 J/kg °C
Thermal conductivity	2.0 W/m °C
Initial conditions	
pressure	60.0 bar
temperature	275.55 °C
gas saturation	0.01
Well	
radius	0.2 m (≈ 8 inch)
wellhead pressure	7.0 bar
feed zone depth	1000 m

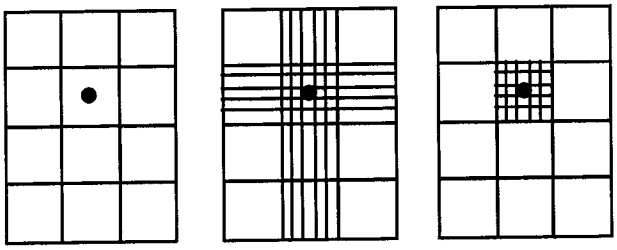

Figure 1. Grid refinement near a production well, indicated by a solid circle. A coarse grid (a) is refined globally (b) and locally (c).

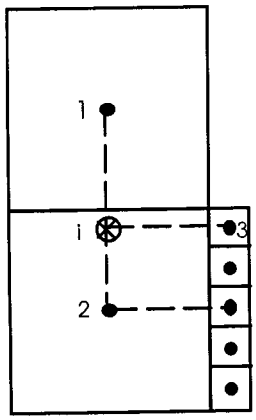

Figure 2. Enlarged view of upper left portion of the locally refined grid in Fig. 1c.

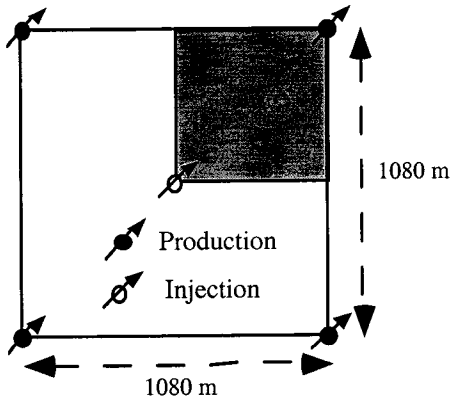

Figure 3. Five-spot well pattern, showing a 1/4 symmetry domain.

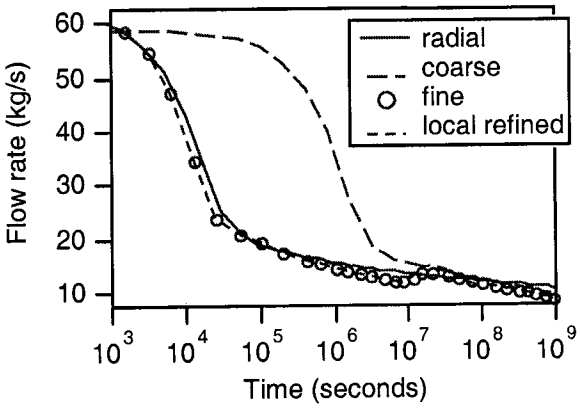

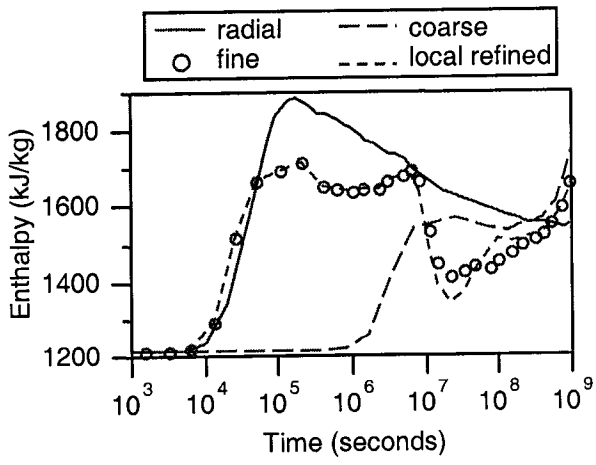

Figure 5. Flow rate (top) and enthalpy transients (bottom) in a hot two-phase reservoir.

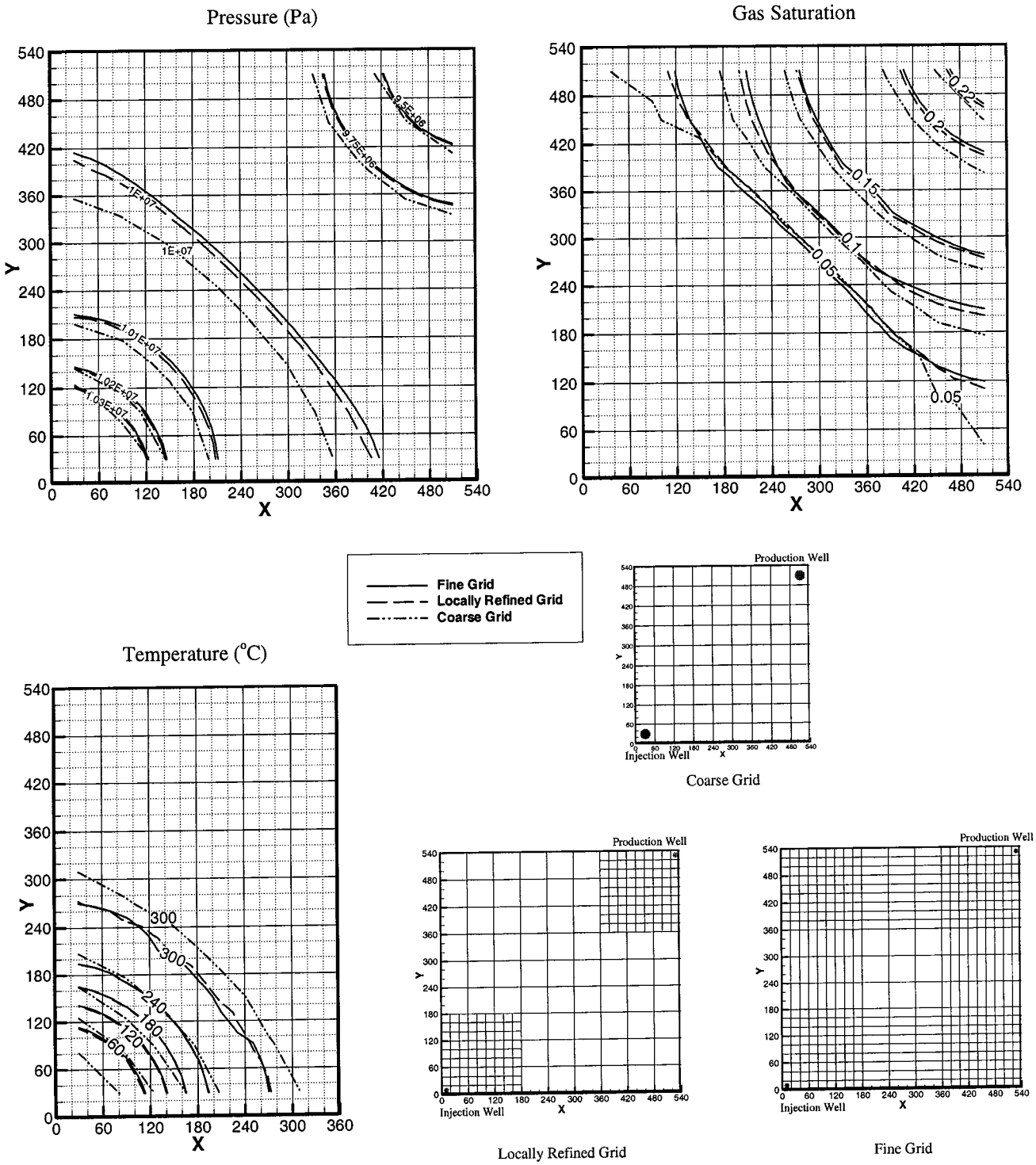

Figure 4. Simulated pressures (a), gas saturations (b) and temperatures (c) after 2 years of simulation time. The different grids are also shown.